Crystal Capture and Settling in Silicic Magma Chambers Consisting of a Eutectic Melt and Pre-existing Crystals II: Two-dimensional Simulation

Koshi NISHIMURA*

Abstract

Many granitic plutons possess a concentrically zoned structure that grades into a more silicic core (i.e., a normally zoned structure) or mafic core (a reversely zoned structure). This zoning has been interpreted to provide evidence of change in magma composition over multiple emplacement events. Here, it is demonstrated that these features can also be generated by the capture of crystals by a solidifying magma crust.

This study numerically models the effect of the settling of pre-existing crystals on the compositional structure of a silicic magma chamber. The modeling assumes a two-dimensional magma chamber consisting of 20 vol% pre-existing crystals and a eutectic melt with a melt viscosity of 10^8, 10^6 and 10^4 Pa s. The distribution of pre-existing crystals is controlled by the balance of the rate of crystal settling and the migration rate of the solid wall (i.e., the capture front within the magma chamber).

A magma chamber with a melt viscosity of 10^8 Pa s yields an almost homogeneous distribution of pre-existing crystals throughout the cooling history of the chamber, primarily because the migration rate of the capture front is much higher than the rate of crystal settling. In comparison, the cooling of a chamber with a melt viscosity of 10^6 Pa s involves crystal capture and settling processes that form concentrically zoned structures that include (1) shallow-level normally zoned structures and (2) deeper-level reversely zoned structures. Finally, a magma chamber with a melt viscosity of 10^4 Pa s develops a vertically zoned structure over a short period of time. In general, vertically zoned structures develop within rhyolitic magma chambers whereas concentrically zoned structures develop in granitic magma chambers; this difference is primarily the result of the viscosity difference between granitic and rhyolitic melts.

1. Introduction

Silicic magmas consisting of a eutectic (or minimum) melt and pre-existing crystals

*）Natural Science Laboratory, 5-28-20 Hakusan, Bunkyo-ku, Tokyo 112-8606

(i.e., restites or early formed phenocrysts) have been emplaced within the continental crust throughout geological history (White and Chappell, 1977; Wyborn and Chappell, 1986; Chappell et al., 1987). The magma chambers that form during emplacement undergo crystallization that is confined to a solid–magma boundary that is analogous to an ice–water transition (Nishimura, 2006, 2015). The presence of a homogeneously dense (both thermally and compositionally) liquid means that convective motion within the chamber is suppressed (Nishimura 2006). This in turn means that the compositional evolution of the final solidified silicic magma chamber (i.e., a granitic intrusion) is governed solely by the interaction of the movement of the solidifying crust (or capture front) generated by the migrating crystallization of the melt within the chamber and the settling of pre–existing crystals.

Marsh (1988) studied the thermal and compositional evolution of a static magma in a sheet–like chamber and found that: (1) a downward–solidifying crust of magma might overtake slowly settling crystals, capture them, and incorporate them into the crust itself if the growth rate of the leading edge of the capturing crust (hereafter termed the capture front) is higher than the rate of crystal settling; (2) the growth of this crust slows systematically with time, capturing fewer and fewer crystals; and (3) the concentration of pre–existing crystals decreases downward within the chamber before increasing as a result of basal accumulation. This capturing process has been used to explain the S–shaped vertical distribution of captured crystals that is present within many sheet–like mafic bodies (Gray and Crain, 1969; Fujii, 1974; Marsh, 1988, 1989, 1996; Mangan and Marsh, 1992). More recently, Nishimura (2015) proposed a one–dimensional crystal capture model for sheet–like silicic magma chambers containing eutectic melt and pre–existing crystals. This modeling indicated that the vertical concentration of captured crystals changes linearly and that a clear compositional gap develops at certain depths within the chamber. This study expands this model to a two–dimensional magma chamber in order to investigate the effects of side–wall crystallization on the development of compositional structures. The implications of the results for the compositional structures known to be present within granitic plutons and rhyolitic magma chambers are examined.

2. Model and assumptions

The modeling is based on a two–dimensional magma chamber consisting of a eutectic melt and 20 vol% pre–existing crystals. These crystals are spherical, are uniformly sized, and are initially distributed homogeneously throughout the 1×1 km magma chamber. The initial temperatures of the magma and the surrounding rock are assumed to be 700℃ and 150℃, respectively, with the former assumed to be the eutectic tem-

perature of the magma. Constant temperature boundaries (T_∞ = 150℃) are distal (5 km) from the magma body so that these constant temperatures do not influence the thermal evolution of the magma chamber.

Eutectic melts crystallize at a single temperature (e.g., Huppert and Sparks, 1988) with crystallization confined to a solid–magma boundary analogous to the ice–water transition (known as the Stefan problem). This solid–magma boundary corresponds to the capture front of Marsh (1988), which moves progressively inward and captures slowly settling crystals. The crystalline products of the eutectic melt are compositionally identical to the melt, and the magma chamber does not undergo any convective motion, as both Ra and Rs are equal to zero. Consequently, the formation of any compositional structure within the magma chamber is governed solely by a balance between the migration of the capture front and the settling of pre–existing crystals. The migration rate of capture front is also related to the degree of crystal settling within the chamber; for example, the Stefan solidification problem is characterized by a capture front migration rate that is inversely proportional to the heat of crystallization (e.g., Turcotte and Schubert, 1982). The increase in the volume of pre–existing crystals reduces the volume of liquid and hence also reduces the released heat of solidification derived from the magma. This indicates that the accumulation of pre–existing crystals increases the migration rate of the capture front within the accumulated section of the chamber. However, the degree of crystal settling is also strongly controlled by the migration rate of the capture front, primarily as fast–moving capture fronts capture suspended crystals before they can undergo gravitational settling. This means that the interdependent relationship between these parameters needs to be incorporated into any modeling of magma chamber processes.

Stokes' Law indicates that the terminal settling velocity (V) of a spherical particle (a pre–existing crystal in this case) in a diluted suspension is

$$V = \frac{a^2 g \Delta\rho}{18\eta} \tag{1}$$

where a is the diameter of the particle, g is acceleration due to gravity, $\Delta\rho$ is the density contrast between the particle and the liquid, and η is the shear viscosity of the liquid. This equation is only valid for a magma containing $<$0.01 vol% crystals (Schwindinger, 1999). The settling velocity of a particle in a concentrated suspension is generally less than the Stokes' velocity (Lockett and Al–Habbooby, 1973, 1974; Mirza and Richardson, 1979; Greenspan and Ungarish, 1982; Selim et al., 1983; Al–Naafa and Selim, 1992; Hoyos et al., 1994), partly because the downward movement of particles causes an equal volumetric flow of displaced fluid in the opposite direction to particle settling. In addition, the average velocity gradients (and shear stress) at a given relative

velocity is greater in more concentrated suspensions. Particles of uniform size and density should settle at equal velocities (barring small statistical variations), meaning that there will be few interparticle collisions or near-collisions between settling particles (Mirza and Richardson, 1979). Richardson & Zaki (1954) proposed that particles settle according to the following formula:

$$V_s = V(1-\phi_0)^N \tag{2}$$

where ϕ_0 is the modal fraction of the particles in a suspension and N is an empirically determined constant that varies between 4.6 (Mirza and Richardson, 1979) and 6.55 (Al-Naafa and Selim, 1992). This study tentatively assumes an N values of 5, a ϕ_0 value of 0.2, and a settling velocity that is constant throughout the magma chamber. An upward-solidifying crust (i.e., a solid floor) is also present within the model; this floor captures settling crystals unless the concentration of captured crystals (ϕ_E) reaches the critical fraction value (ϕ_{crit}) that is needed for packing (Nishimura, 2006, 2015). When ϕ_E reaches ϕ_{crit}, a settling layer of cumulus crystals and intercumulus liquid develops on the solid floor. The critical packing fraction of crystals, ϕ_{crit}, is assumed to be 0.6 (i.e., maximum concentration of pre-existing crystals is 60 vol%).

The heat conduction between the magma and the surrounding rock or the solidified part of the magma chamber can be expressed as follows:

$$\rho c \frac{\partial T}{\partial t} = \lambda\left(\frac{\partial^2 T}{\partial x^2} + \frac{\partial^2 T}{\partial y^2}\right) \tag{3}$$

where ρ is density, c is specific heat, λ is thermal conductivity, and T is temperature. The interior of the magma body does not undergo heat flow as it has a homogeneous temperature and is not undergoing crystallization. In comparison, heat flows do occur at the solid-magma boundary, meaning that crystallization is confined to this boundary. The solid-magma boundary migrates inward similar to an ice-water boundary, and the energy balance at the solid-magma boundary can be described as follows:

$$\rho L(1-\phi_E)V_B = -\lambda(\nabla T \cdot n) \tag{4}$$

where L is the latent heat of crystallization, ϕ_E is the concentration of captured crystals, V_B is the migration rate of the solid-magma boundary, and n is the outward normal vector from this boundary. The values for the physical parameters adopted in this study are as follows: $g = 9.8$ m s^{-2}, $a = 6.0\times10^{-3}$ m, $\Delta\rho = 0.5\times10^3$ kg m^3, $\eta = 10^4$–10^8 Pa s, $\lambda = 2.4$ W m^{-1}, $c = 1.3\times10^3$ J kg^{-1}, and $L = 2.9\times10^5$ J kg^{-1}.

The modeled region was divided into 10×10 m square cells to enable finite difference

numerical calculations. The volume fractions of pre-existing crystals within each cell were calculated using Eqs 1 and 2 for each time step. The onset of crystallization in a cell means that the pre-existing crystal fraction within this cell becomes fixed (i.e., the pre-existing crystals are captured). This fraction of pre-existing crystals is related to the duration of solidification, a process that is further discussed by Nishimura (2006, 2015). Cells with smaller fractions of pre-existing crystals undergo longer-duration solidification, primarily as a result of the large amount of released heat during crystallization (Eq. 4).

The rate of crystal settling is strongly controlled by melt viscosity, and experimental studies indicate that the viscosity of natural silicic melts generated at a given crustal pressure is largely independent of temperature (Scaillet et al., 1998). In particular, the eutectic (or minimum) melt on the water-saturated solidus at a given pressure must have a constant viscosity because major element concentrations (including H_2O) and temperatures are constant throughout the solidification of the melt. Nishimura (2015) estimated the viscosities of the water-saturated eutectic (or minimum) melts from haplogranite data presented by Tuttle and Bowen (1958) and Holtz et al. (1992). With a decrease in pressure from 500 to 50 MPa, the H_2O content of a eutectic melt decreases from 9.9 to 2.4 wt% and the viscosity increases from 10^4 to 10^8 Pa s. The modeling undertaken during this study calculates the distribution of pre-existing crystals for magmas with constant melt viscosities of 10^8, 10^6, and 10^4 Pa s.

4. Results

The thermal and compositional evolution of a magma chamber generated by settling of pre-existing crystals was calculated for melt viscosities of 10^8, 10^6, and 10^4 Pa s (Figs. 1-3). The distribution of pre-existing crystals represents a compositional structure, as the composition of pre-existing crystal and the co-existing eutectic melt corresponds to the mafic and silicic end-members of the system, respectively. The thermal structures and spatial variations in the distribution of pre-existing crystals in a system with a melt viscosity of 10^8 Pa s are shown for different time periods in Fig. 1. This model indicates that the solidification rate is much higher than the rate of crystal settling throughout the cooling history of the magma chamber, primarily as the high melt viscosity inhibits crystal settling. This indicates that almost all of the pre-existing crystals are incorporated into the solidifying crust with minimal movement. This process maintains the almost homogeneous distribution of pre-existing crystals throughout the cooling history and generates a more homogeneous pluton suite (Fig. 1f) than is the case for lower-viscosity melts (Figs 2f and 3d). In this model the center of the thermal structure is almost invariant throughout cooling (Fig. 1a, c, and d) because the homogeneous distribution of

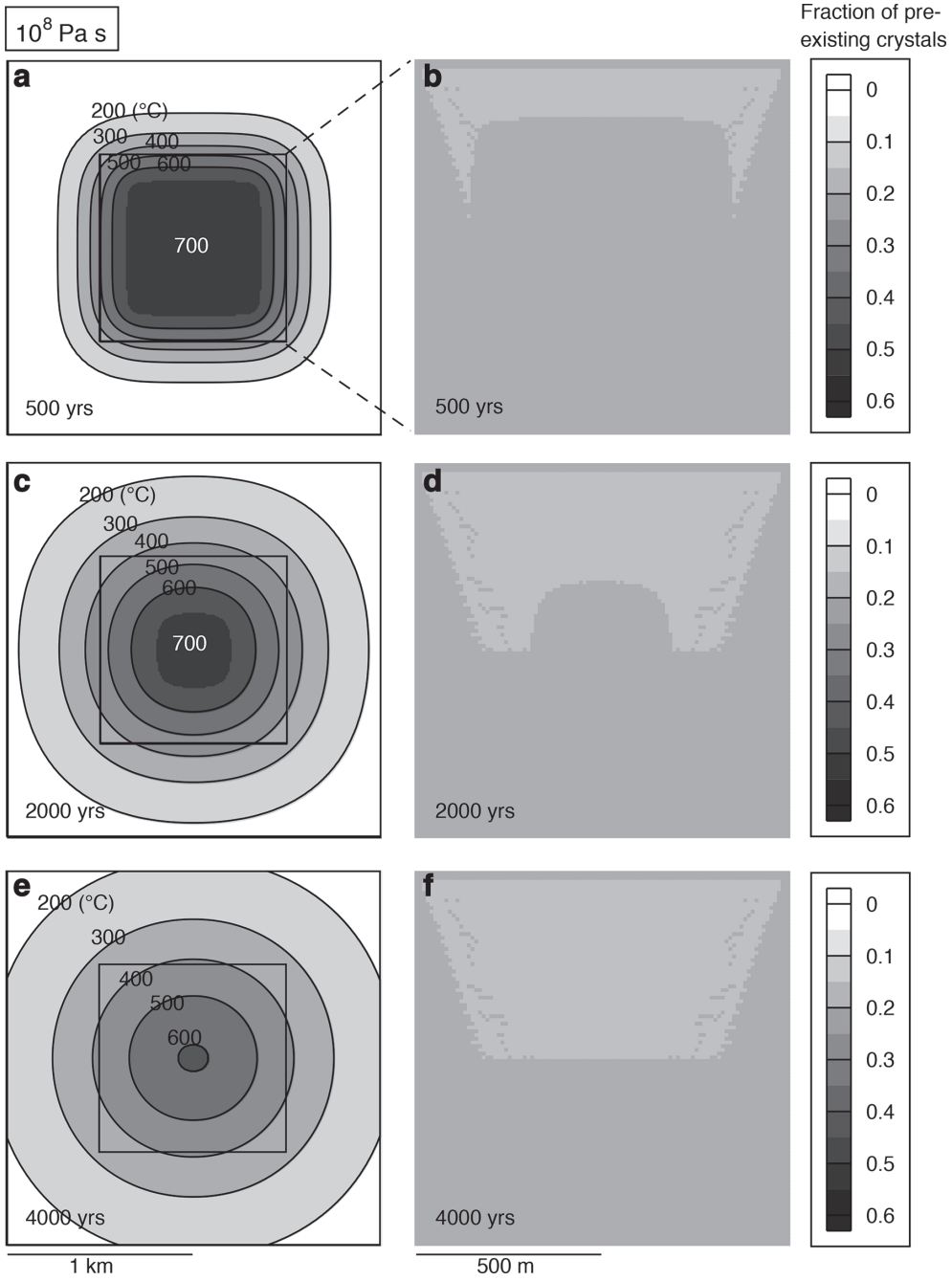

Fig. 1. Thermal structure (a, c, and e) and the distribution of pre-existing crystals (b, d, and f) within a magma chamber with a melt viscosity of 10^8 Pa s. Squares in a, c, and e show the initial shape of the magma chamber, and the region with a temperature of 700°C indicates the area containing magma.

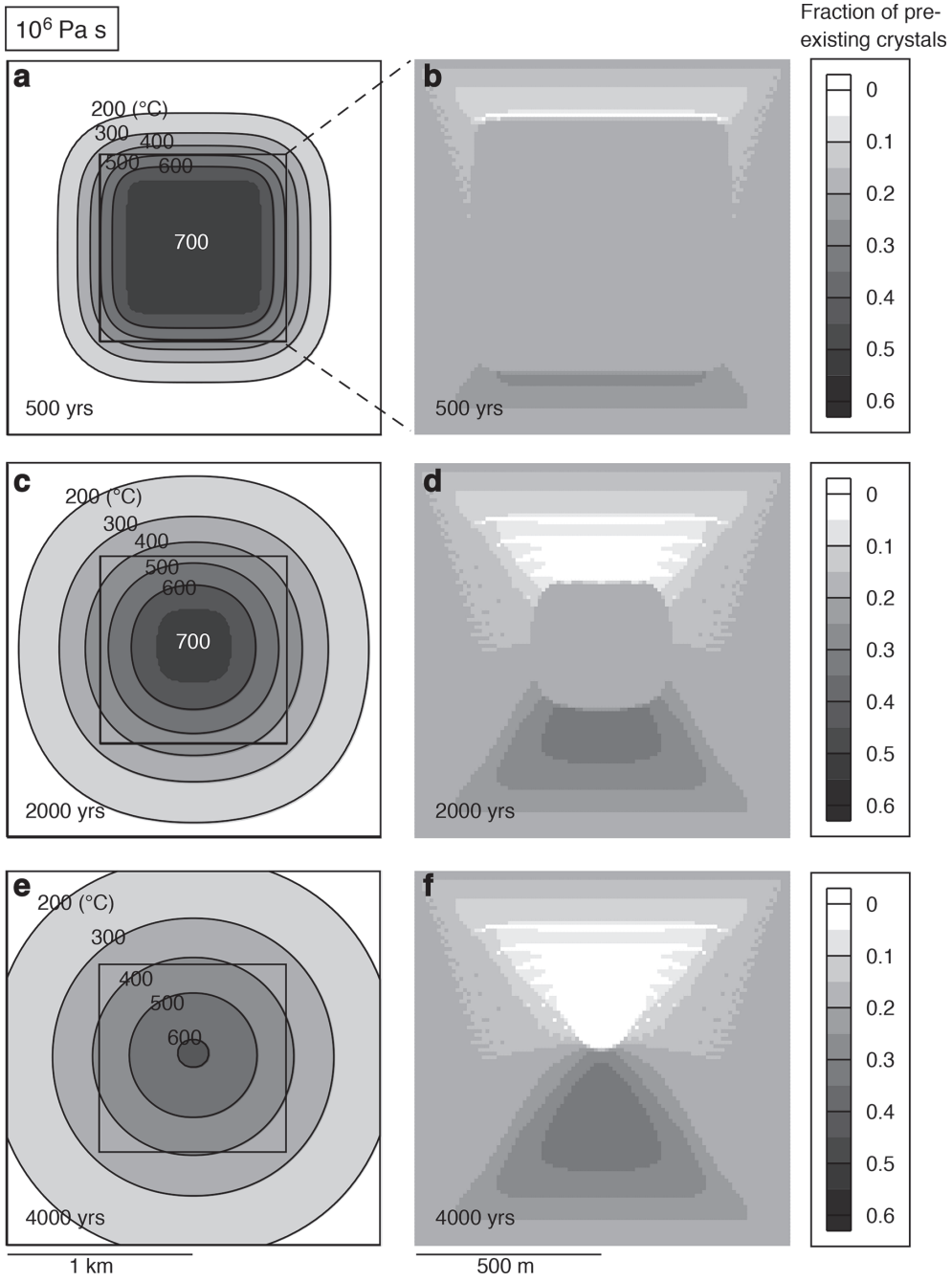

Fig. 2. Thermal structure (a, c, and e) and the distribution of pre-existing crystals (b, d, and f) within a magma chamber with a melt viscosity of 10^6 Pa s. Squares in a, c, and e show the initial shape of the magma chamber, and the region with a temperature of 700°C indicates the area containing magma.

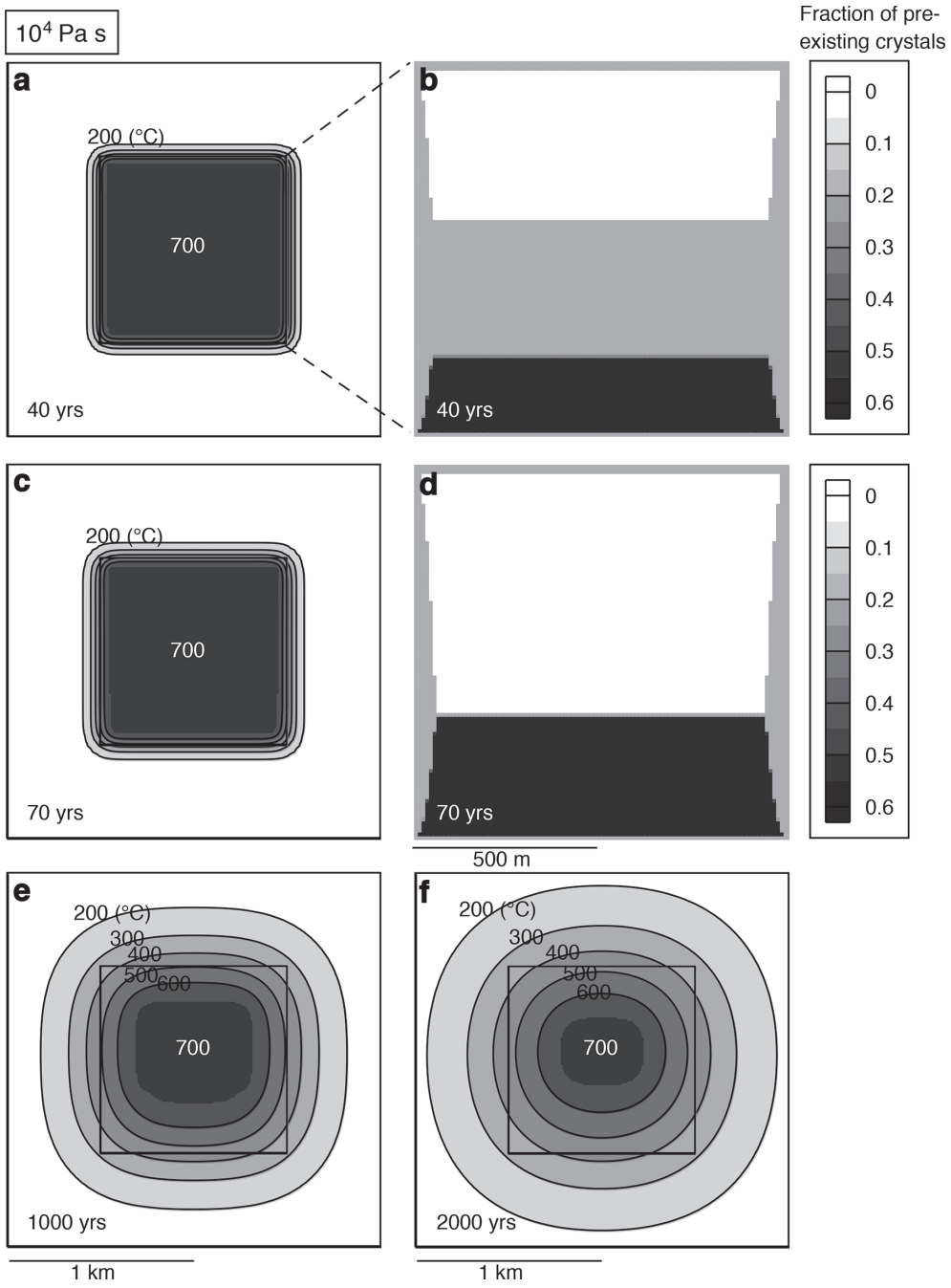

Fig. 3. Thermal structure (a, c, e, and f) and the distribution of pre-existing crystals (b and d) within a magma chamber with a melt viscosity of 10^4 Pa s. Squares in a, c, e, and f show the initial shape of the magma chamber, and the region with a temperature of 700℃ indicates the area containing magma.

melt within the chamber yields a homogeneous release of latent heat of crystallization within the system.

Modeling of a chamber containing melt with a viscosity of 10^6 Pa s yields a migration rate of solidification front that is initially higher than the rate of crystal settling but becomes lower over time. The downward-growing roof zone has an initial rate of solidification that is higher than the rate of crystal settling, indicating that this zone incorporates a significant volume of pre-existing crystals during the early stages of cooling of the chamber (Fig. 2b). The latest stages of cooling are associated with a systematic slowing of the expansion of the capture front with time as the thermal gradient around the magma chamber decreases (Fig. 2a, c, and e). This eventually leads to a decrease in the concentration of captured pre-existing crystals with depth until the value equals zero. In comparison, the upward-migrating floor zone captures pre-existing crystals without accumulation during the early stages of cooling of the chamber, and the rate of the migration of this zone systematically decreases with time, although the concentration of pre-existing crystals increases upward as a result of basal accumulation within the chamber. The sidewalls of the chamber also continuously freeze these processes of crystal settling throughout the cooling of the chamber. All of these processes yield a normally zoned structure with an external mafic zone and internal silicic zone in the shallow part of the chamber and a reversely zoned structure with a silicic outer zone and a mafic inner zone at the deeper levels (Fig. 2f). The rate of solidification of the crystal-rich (i.e., cumulative) part of the chamber is higher than the rate of the solidification of the crystal-poor part of the chamber, as the former releases a smaller amount of heat during crystallization. This indicates that the center of the thermal structure (i.e., center of the magma chamber) shifts slightly upward over time (Fig. 2a, c, and e).

A magma chamber containing melt with a viscosity of 10^4 Pa s has a rate of crystal settling that is far higher than the rate of solidification. This indicates that crystal settling proceeds rapidly, resulting in a vertically zoned chamber in which the magma becomes more silicic with increasing height (Fig. 3b). The basal accumulation of crystals is completed over only a short time scale (about 70 years), coincident with the fixing of the distribution of pre-existing crystals (Fig. 3d). The rate of solidification of the cumulative part of the chamber (40 vol.% liquid) is much higher than the rate of the solidification of the crystal-free part (100 vol.% liquid), primarily as the former releases much smaller amounts of crystallization-derived heat. This result indicates that the center of the magma body shifts markedly upward over time (Fig. 3a, c, e, and f). In addition, some 2000 years of crystallization yields a scenario where the thermal gradient in the region below the magma body is smaller than the gradient in the region above (Fig. 3f), primarily as a result of the rapid upward movement of the base of the magma body.

5. Implications for petrology

The results of the numerical modeling outlined above indicate that the compositional structure of silicic magma chambers is strongly controlled by the viscosity of melt within the chamber, a variable that shows a marked decrease with increasing depth and melt H_2O content. Petrological analysis suggests that silicic volcanic ejecta have pre-eruptive melt viscosities of $10^5 - 10^4$ Pa s irrespective of temperature (Scaillet et al., 1998). The modeling presented here indicates that crystal settling within a rhyolitic magma chamber ($\sim 10^4$ Pa s) will occur immediately to form a vertically zoned structure (Fig. 3b and d), consistent with the observation that many rhyolitic magmas are erupted from vertically zoned magma chambers (e.g., Ewart, 1965; Lipmann et al., 1966; Birch, 1978; Hildreth, 1979; Nakada, 1983).

In comparison, many granitic suites are not associated with vertically zoned structures but instead are associated with concentrically zoned structures and zoned plutons (e.g., Bateman and Nokleberg, 1978; Gastil et al., 1991; Nishimura and Yanagi, 2000). These plutons are either (1) normally zoned, where the least differentiated phases are located at the margin of the pluton before becoming successively more differentiated towards the interior, or are (2) reversely zoned plutons, which have differentiated margins and more mafic interiors. Granitic melt viscosities and H_2O contents are difficult to determine, primarily as these magmas preserve few melt inclusions, but can be roughly estimated using compositional structures. The modeling presented here indicates that magma chambers with melt viscosities of 10^6 Pa s generate normally zoned structures at shallow levels that give way to reversely zoned structures at deeper levels within a single chamber (Fig. 2f). This model is consistent with the presence of these two types of zoned plutons within the geological record, as exposed granitic suites have almost always undergone some level of erosion. Even if the eutectic (or minimum) melt is water-undersaturated, this melt has a viscosity that is almost equal to that of a water-saturated eutectic (or minimum) melt at the same pressure (Hess and Dingwell, 1996; Scaillet et al., 1996, Holtz et al., 2001, Nishimura, 2006). This indicates that the modeling presented here (Figs 1–3) can also be considered indicative of the processes that affect water-undersaturated high-silica magmas.

Petrological research indicates that some rhyolitic volcanic rocks were erupted from the upper parts of magma chambers that then go on to crystallize and form granitic plutons (e.g., Bachmann et al., 2007). This indicates that rhyolites and granites that form from silicic magma chambers with melt viscosities greater than 10^7 Pa s (i.e., in the shallow parts of the crust) have almost the same composition as each other (Fig 3; also see Nishimura, 2015). In comparison, crystal-poor rhyolites and crystal-rich cumulative granites form from magmas containing melts with viscosities of $< 10^5$ Pa s (i.e., at deeper levels within the crust; Nishimura 2015). The melt viscosities of extrusive magmas

rarely exceed 10^6 Pa s, suggesting that any magmas with melt viscosities of $>10^6$ Pa s cannot leave their host magma chamber and inevitably freeze at depth (Scaillet et al., 1998). The results of this study suggest that rhyolitic magmas generally erupt from deeper levels within the crust than the typical emplacement level of zoned granitic plutons.

Acknowledgements

I would like to thank T. Nishiyama and T. Kawamoto for valuable discussions and encouragement during this research. I am also indebted to T. Yanagi, T. Ikeda and T. Miyamoto for valuable advice during this study.

References

Al-Naafa, M. A., and Selim, M. S. (1992) Sedimentation of monodisperse and bidisperse hard-sphere colloidal suspensions. *AIChE J.,* 38(10), 1618-1630.

Bachmann, O., Miller, C. F., and de Silva, S. L. (2007) The volcanic-plutonic connection as a stage for understanding crustal magmatism. *J. Volcanol. Geotherm. Res.,* 167, 1-23.

Bateman, P. C., and Nokleberg, W. J. (1978) Solidification of the Mount Givens Granodiorite, Sierra Nevada, California. *J. Geol.* 86, 563-579.

Birch, W. D. (1978) Petrogenesis of some Paleozoic rhyolites in Victoria. *J. Geol. Soc. Aust.,* 25, 75-87.

Chappell, B. W., White, A. J. R., and Wyborn, D. (1987) The importance of residual source material (restite) in granite petrogenesis. *J. Petrol.,* 28, 1111-1138.

Ewart, A. (1965) Mineralogy and petrogenesis of the Whakamaru ignimbrite in the Maraetai area of the Taupo volcanic zone, New Zealand. *N. Z. J. Geol. Geophys.* 8, 611-677.

Fujii, T. (1974) Crystal settling in a sill. *Lithos,* 7, 133-137.

Gastil, G., Nozawa, T., and Tainosho, Y. (1991) The tectonic implications of asymmetrically zoned plutons. *Earth Planet. Sci. Lett.* 102, 302-309.

Gray, N. H., and Crain, I. K. (1969) Crystal settling in sills: A model for suspension settling. *Can. J. Earth Sci.,* 6, 1211-1216.

Greenspan, H. P., and Ungarish, M. (1982) On hindered settling of particles of different sizes, *Inter. J. Multi. Flow* 8, 587-604.

Hess, K. U., and Dingwell, D. B. (1996) Viscosities of hydrous leucogranitic melts: a non-Arrhenian model. *Am. Mineral.,* 81, 1297-1300.

Hildreth, W. (1979) The Bishop Tuff: evidence for the origin of compositional zonation in

silicic magma chambers. *Spec. Pap. Geol. Soc. Am.,* 180, 43–75.

Holtz, F., Johannes, W., Tamic, N., and Behrens, H. (2001) Maximum and minimum water contents of granitic melts generated in the crust: a reevaluation and implications. *Lithos,* 56, 1–14.

Holtz, F., Pichavant, M., Barbey, P., and Johannes, W. (1992) Effects of H_2O on liquidus phase relations in the haplogranite system at 2 and 5 kbar. *Am. Mineral.,* 77, 1223–1241.

Hoyos, M., Bacri, J. C., Martin, J., and Salin, D. (1994) A Study of the sedimentation of noncolloidal bidisperse, concentrated suspension by an acoustic technique. *Phys. Fluids* 6(12), 3809–3817.

Huppert, H. E., and Sparks, R. S. J. (1988) The generation of granitic magmas by intrusion of basalt into continental crust. *J. Petrol.* 29, 599–642.

Lipman, P. W., Christiansen, R. L., and O'Connor, J. T. (1966) A compositionally zoned ash-flow sheet in southern Nevada. *Prof. Pap. U.S. Geol. Surv.* 524-F.

Lockett, M. J., and Al-Habbooby, H. M. (1973) Differential settling by size of two particle species in a liquid. *Trans. Inst. Chem. Eng.* 51, 281–292.

Lockett, M. J., and Al-Habbooby, H. M. (1974) Relative particle velocities in two-species settling. *Powder Technol.* 10, 67–71.

Mangan, M. T., and Marsh, B. D. (1992) Solidification front fractionation in phenocryst-free sheet-like magma bodies. *J. Geol.,* 100, 605–620.

Marsh, B. D. (1988) Crystal capture, sorting and retention in convecting magma. *Geol. Soc. Am. Bull.,* 100, 1720–1737.

Marsh, B. D. (1989) Magma chambers. *Ann. Rev. Earth Planet. Sci.,* 17, 4395–474.

Marsh, B. D. (1996) Solidification fronts and magmatic evolution. *Mineral. Mag.,* 60, 55–40.

Mirza, S., and Richardson, J. F. (1979) Sedimentation of suspensions of particles of two or more sizes. *Chem. Eng. Sci.,* 34, 447–454.

Nakada, S. (1983) Zoned magma chamber of the Osuzuyama acid rocks, southwest Japan. *J. Petrol.* 24, 471–494.

Nishimura, K., and Yanagi, T. (2000) In situ crystallization observed in the Osumi granodiorite batholith. *Earth Planet. Sci. Lett.* 180, 185–199.

Nishimura, K. (2006) Numerical modeling of trace element behavior during crystal settling and reequilibration in high-silica magma bodies. *J. Geophys. Res.,* 111: B08201. doi:10.1029/2005JB003844

Nishimura, K. (2015) Crystal capture and settling in sheet-like silicic magma chambers consisting of eutectic melt and pre-existing crystals. *J. Toyo Univ. (Nat. Sci.),* 59, 35–46.

Richardson, J. F., and Zaki, W. N. (1954) Sedimentation and fluidization. Part I. *Trans. Inst. Chem. Eng.,* 32, 35–53.

Scaillet, B., Holtz, F., Pichavant, M., and Schmidt, M. O. (1996) The viscosity of Himalayan leucogranites: implications for mechanisms of granitic magma ascent. *J. Geophys. Res.,* 101, 27691–27699.

Scaillet, B., Holtz, F., and Pichavant, M. (1998) Phase equilibrium constraints on the viscosity of silicic magmas. *J. Geophys. Res.,* 103, 27257–27266.

Selim, M. S., Kothari, A. C., and Turian, R. M. (1983) Sedimentation of multisized particles in concentrated suspensions. *AIChE J.* 29, 1029–1038.

Turcotte, D. L., and Schubert, G. (1982) *Geodynamics,* John Wiley & Sons, New York, 450pp.

Tuttle, O. F., and Bowen, N. L. (1958) Origin of granite in the light of experimental studies in the system $NaAlSi_3O_8-KAlSi_3O_8-SiO_2-H_2O$. *Geol. Soc. Am. Mem.,* 74.

White, A. J. W., and Chappell, B. W. (1977) Ultrametamorphism and granitoid genesis. *Tectonophisics,* 43, 7–22.

Wyborn, D., and Chappell, B. W. (1986) The petrogenetic significance of chemically related plutonic and volcanic rock units. *Geol. Mag.,* 123, 619–628.

要旨

珪長質マグマ溜まりの固化前線における沈降結晶の捕獲 Ⅱ：2次元シミュレーション

西村　光史*

共融点メルトと浮遊結晶からなる2次元珪長質マグマ溜まりを仮定し、固化前線による沈降結晶の捕獲が組成の空間構造にもたらす影響について計算を行った。マグマ溜まりの深度に応じて共融点メルトの粘性は大きく変化する。メルト粘性が10^8 Pa sの場合、結晶沈降速度を固化速度が大きく上回るため、冷却史を通じてほぼ均一な組成構造が保たれる。メルト粘性が10^6 Pa sの場合、マグマ溜まりの浅部に同心状の正累帯構造(中心が珪長質)が形成され、深部に逆累帯構造(中心が苦鉄質)が形成される。メルト粘性が10^4 Pa sの場合、結晶沈降が速やかに進行し、重力方向に分化した組成構造を形成する。